Dear Author,

Please, note that changes made to the HTML content will be added to the article before publication, but are not reflected in this PDF.

Note also that this file should not be used for submitting corrections.

RSC Advances c4ra15739g

PAPER

1

Efficient alignment of primary CNS neurites using structurally engineered surfaces and biochemical cues

Munyaradzi Kamudzandu, Ying Yang, Paul Roach and Rosemary A. Fricker

Micro- and nano-structured materials were used to investigate directional alignment of primary CNS neurons (red) co-cultured with astrocytes (green).

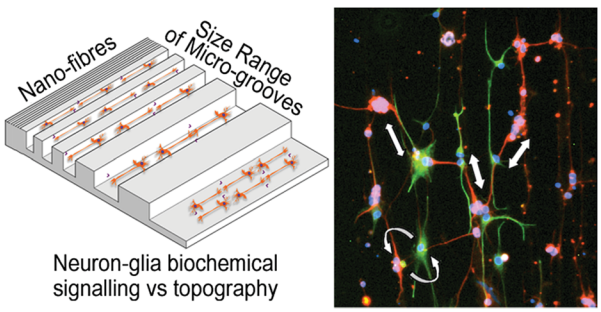

Please check this proof carefully. **Our staff will not read it in detail after you have submitted your proof corrections.**

Translation errors between word-processor files and typesetting systems can occur so the whole proof needs to be read. Please pay particular attention to: tabulated material; equations; numerical data; figures and graphics; and references. If you have not already indicated the corresponding author(s) please mark their name(s) with an asterisk. Corrections at this stage should be minor and not involve extensive changes. Please do not directly edit the text within the PDF file or send a revised manuscript. All corrections must be submitted at the same time.

Please bear in mind that minor layout improvements, e.g. in line breaking, table widths and graphic placement, are routinely applied to the final version.

We will publish articles on the web as soon as possible after receiving your corrections; **no late corrections will be made.**

Please return your **final** corrections, where possible within **48 hours** of receipt following the instructions in the proof notification email.

Queries for the attention of the authors

Journal: RSC Advances

Paper: c4ra15739g

Title: Efficient alignment of primary CNS neurites using structurally engineered surfaces and biochemical cues

Editor's queries are marked like this... 1, and for your convenience line numbers are inserted like this... 5

Please ensure that all queries are answered when returning your proof corrections so that publication of your article is not delayed.

Query Reference	Query	Remarks
1	For your information: You can cite this article before you receive notification of the page numbers by using the following format: (authors), RSC Adv., (year), DOI: 10.1039/c4ra15739g.	
2	Please carefully check the spelling of all author names. This is important for the correct indexing and future citation of your article. No late corrections can be made.	
3	Do you wish to indicate the corresponding author(s)? If so, please specify the corresponding author(s).	

RSC Advances

PAPER

Efficient alignment of primary CNS neurites using structurally engineered surfaces and biochemical cues†

Cite this: DOI: 10.1039/c4ra15739g

Munyaradzi Kamudzandu,[a] Ying Yang,[b] Paul Roach[b] and Rosemary A. Fricker[a]

Received 3rd December 2014
Accepted 19th February 2015

DOI: 10.1039/c4ra15739g

www.rsc.org/advances

Tissue engineering strategies for the central nervous system (CNS) have been largely hampered by the complexity of neural cell interactions and limited ability to control functional circuit formation. Although cultures of primary CNS neurons give key insight into an *in vivo* state, these cells are extremely sensitive to local micro-environments and are therefore often replaced with cell lines. Here we aimed to combine primary CNS neurons with surface nano- and micro-topography, and biochemical cues, to direct neurite outgrowth. Neurons were cultured on nano-fibers and micro-grooves either coated with poly-L-lysine and laminin (PLL–LN) or pre-seeded with naturally supporting astrocyte cells. Developing neurites extended parallel to PLL–LN coated topography, significantly more on micro-grooved than nano-fiber substrata. Astrocytes were found to direct neurite alignment to a greater extent compared to structured surface cues, highlighting the importance for biochemical signalling and cellular architecture. Equally neuron–neuron interactions strongly influenced neurite outgrowth. On micro-structured surfaces neurite orientation was regulated by contact guidance cues at the edges of grooves. All of our findings show that we can control the behaviour of primary CNS neurons *in vitro* using surface engineering approaches. This will allow us to establish neuronal circuitry, to model neurodegenerative diseases and advance regenerative medicine strategies.

Introduction

The potential of regenerative medicine has not yet been fully translated into clinical delivery due to a lack of understanding of complex biological systems and a limited ability to convey control over engineered tissues. In particular, within the nervous system neuronal architecture is highly complex, allowing multiple cross-communication between a plethora of cell types; this has limited the development of successful clinical interventions, being particularly pertinent for the central nervous system (CNS). For example, the basal ganglia circuitry of the brain is made up of five interconnected subsets of neurons and is mainly responsible for controlling movement.[1] Loss of specific neurons in this circuitry leads to the neurodegenerative diseases such as Parkinson's (PD) and Huntington's (HD) diseases.[2] Recreating the precise excitatory and inhibitory connections between the basal ganglia neurons is critical for developing accurate *in vitro* models of PD and HD to test emerging cell and gene therapies.

Materials engineering efforts to steer neural circuit formation rely heavily on the attachment of neurons and directed alignment of their processes (both axons and dendrites).[3] During development, axons from newly differentiated neurons navigate to specific target sites with the aid of growth cones located at their tips.[4] Highly motile filopodia (finger-like structures on growth cones) sense, *via* their receptors, and respond to long or short-range, attractive or repulsive extracellular guidance cues.[5]

The supporting glial cells in the CNS provide topographical and biological cues for axonal path-finding *in vivo*.[6] Phillips *et al.*, have demonstrated the use of pre-seeded astrocyte materials to steer the alignment and elongation of subsequently added neurons.[7] Others have reported similar characteristics for cells from the peripheral nervous system with axonal growth orientating parallel to aligned astrocytes.[8,9]

In addition to directional cues imposed by chemoattraction or chemorepulsion, other important cues are involved during development of the CNS. Adhesive cues, such as those received from laminin (LN) and fibronectin in the extracellular matrix (ECM), or cell adhesion molecules expressed by glial cells, generate a micro-environment that is permissive to neuronal attachment and axon extension.[10,11] The ability to regulate axonal orientation and elongation is key to controlling circuit formation; to enable the formation of highly organized neural networks.

[a]*Institute for Science and Technology in Medicine, Keele University, Keele, Staffordshire, ST5 5BG, UK. E-mail: r.a.fricker@keele.ac.uk*

[b]*Guy Hilton Research Centre, Keele University, Thornburrow Drive, Staffordshire, ST4 7QB, UK. E-mail: p.roach@keele.ac.uk*

† Electronic supplementary information (ESI) available. See DOI: 10.1039/c4ra15739g

Cutting-edge fabrication techniques are emerging to deliver materials that present both topographical and (bio)chemical cues, to promote neuronal adhesion and subsequent circuit formation *in vitro*.[12–16] Patterned surfaces can be engineered to provide physical guidance for cell elongation or process orientation. Weiss first described this phenomenon as '*contact guidance*'.[17,18] Due to advances in technology and hence pattern fabrication techniques, patterned substrates can be built and reproduced at high efficiency and reasonably low costs.[19] Fabrication techniques include electrospinning and soft lithography.

Electrospinning uses electrostatic force to generate nano or micro-fiber meshes. The electrostatic force is generated when high voltage is applied to the liquid polymer. A jet of fibers is formed when the force overcomes surface tension inherent in the polymer solution; the liquid (solvent) evaporates producing a mesh of fibers with diameters within the nanometer range.[20–22] Soft lithography is a technique used for generating a pattern on substrates at the micron and submicron scale.[23] The pattern is copied from a master template fabricated *via* photolithography. Photolithography uses light sensitivity to fabricate micro-patterns on a surface. A polymer, commonly polydimethyl-siloxane (PDMS) due to its high optical transparency and good thermal stability, is cast onto the master template and cured by cross-linking linear polymer chains. This produces an elastomer block imprinted with the template design, for instance micro-groove structures.[24] PDMS is commonly used in biomedical micro-electromechanical (Bio-MEMS) systems due to its low cost and biological compatibility in addition to its optical transparency and thermal stability.[25]

Herein, we evaluated the alignment of CNS neurites on fabricated substrata. We fabricated poly(lactic acid) (PLA) nano-fibers and PDMS micro-grooves using electrospinning and soft lithography techniques, respectively. These structures provided contact guidance to developing processes for primary neurons derived from the lateral ganglionic eminence in the basal ganglia. Patterned surfaces were either coupled with biological or (bio)chemical cues, *i.e.* astrocytes or poly-L-lysine and laminin respectively, to promote neuronal adhesion and neurite extension. Micro-groove structures fabricated with groove width ranging from 20–80 μm allowed us to evaluate whether varying groove width would affect neurite alignment. Furthermore, we examined whether neurites emanating from clusters of cell bodies on micro-groove substrates had different alignment tendency compared to those extending from single cell bodies. Our results inform the next generation of materials and constructs for *in vitro* tissue engineering and surgical interventions for neural tissue.

Materials and methods

Fabrication of nano-fiber scaffolds

Aligned nano-fiber meshes were fabricated *via* electrospinning of 2% poly-L,D-lactic acid (PLA: 96% L/4% D; Purac BV, Gorinchem, Netherlands) dissolved in a mixture of dichloromethane and dimethylformamide (7 : 3 volume ratio) following a protocol established in our laboratory.[26] The flow rate of the polymer solution out of an 18G needle ranged from 0.022–0.025 mL min^{-1}. A mobile parallel electrode collector was used to collect aligned nano-fibers (Spellman HV, Pulborough, United Kingdom), charged at a range of ±5.5 kV to ±6.5 kV. Fibers from the collector were transferred to acetate frames (4.5 × 4.5 cm); an aerosol adhesive was used to attach fibers onto frames. Fibers were then anchored to coverslips using silicon glue.

Fabrication of PDMS micro-grooves

PDMS micro-grooves were fabricated *via* soft lithography.[24] Initially, silicon masters with dimensions: groove width ranging from 20–80 μm and depth of 2.2 μm were imprinted onto PMMA (polymethylmethacrylate) templates. A two-part kit consisting of silicone elastomer and curing agent (10 : 1 weight ratio) (Sylgard 184, Dow Corning) was used to prepare the PDMS solution. The solution was left at room temperature for 1 h to get rid of bubbles before casting onto PMMA templates placed in a 6 well plate. The solution was cured at 60 °C for 1 h to form PDMS micro-grooves.

Preparing substrates for cell culture

Silicon glue securing the nano-fibers was allowed to dry for 0.5 h before nano-fiber constructs were placed in square petri dishes and covered with foil paper with small holes drilled on top. The constructs were placed under vacuum ~0.3 mbar for 0.5 h to remove any solvents before cell culture. Constructs were sterilized under UV light for 4.5 min. PDMS micro-grooves were incubated in 100% ethanol for 1 h at room temperature. The constructs were left to dry for a few minutes before they were washed with deionized water (dH_2O) to get rid of any remaining ethanol. Some constructs were pre-coated with 0.1 mg mL^{-1} poly-L-lysine (PLL, Sigma-Aldrich, Dorset, United Kingdom) overnight, followed by three washes in distilled water, and then 10 μg mL^{-1} laminin (LN, Sigma-Aldrich, Dorset, United Kingdom) for approximately 4 h. 13 mm diameter circular glass coverslips were used as positive controls for each experiment. These were sterilized in 100% ethanol and left to dry before they were coated with PLL and LN as above.

Cell culture

Pregnant Sprague-Dawley rats and their embryos, bred in-house at Keele University, were killed by approved Schedule 1 methods, following guidelines from the UK Animals, Scientific procedures Act, 1986 and authorization from Keele University's local ethics committee. The embryos were 15–16 days old (E15–E16), with E0 defined as date of observing vaginal plug. Brain tissue was removed and the lateral part of the ganglionic eminence (LGE) was dissected out.[27]

Tissue pieces were placed into a 1.5 mL Eppendorf containing approximately 1 mL of Dulbecco's Modified Eagle's Medium/Nutrient F-12 Ham's medium (DMEM-F12, Sigma-Aldrich, Dorset, United Kingdom). Tissue pieces were washed twice with DMEM-F12 and placed in 0.1% trypsin (Worthington Biochemical Corp., Reading, UK)/0.05% DNase (Greiner Bio-

One, UK) in DMEM-F12 for 20 minutes. The pieces were then washed three times with DNase solution before they were mechanically triturated into individual cells. The cells were centrifuged at 1200 rpm for 3 minutes. The supernatant was aspirated out and cells were re-suspended in neuronal culture medium. Dissociated cells were counted using a hemocytometer (Fisher Scientific, Loughborough, UK) and their viability checked using trypan blue (Invitrogen, Paisley, UK) before cell culture. Cells were cultured in neuronal culture medium (NCM), which consisted of: 95% neurobasal, 1% fetal calf serum (FCS), 1% Penicillin/Streptomycin/Fungizone (PSF), 1% B27 supplement (all from Invitrogen, Paisley, UK), 10 μM L-glutamine (PAA, UK), 0.45% glucose (Sigma-Aldrich, Dorset, United Kingdom). Seeding density was 20 000 to 30 000 cells suspended in 50 μL of NCM.

Purifying astrocytes and co-culture with neurons

To obtain purified cultures of astrocytes, dissociated cells from E15–E16 LGE tissue were also cultured in T-25 flasks with astrocyte culture medium made of: DMEM-F12, 10% FCS, 1% PSF, 1% B27 supplement (all Invitrogen, Paisley, UK), 10 μM L-glutamine, 0.45% glucose and 10 ng mL^{-1} epidermal growth factor (EGF, human recombinant; R&D Systems). Cells were fed with approximately 2 mL of astrocyte medium every 2 days and the identification of astrocytes was confirmed using immunohistochemistry for glial fibrillary acidic protein (GFAP, see below).

When the astrocytes were approximately 80% confluent, medium was removed and cells were washed once with PBS (Sigma-Aldrich, Dorset, United Kingdom). After washing, cells were incubated in 1 mL of 0.025% trypsin (Invitrogen, Paisley, UK) for approximately 3 minutes; the flask was lightly tapped at the sides to make sure the cells were detached. 4 mL of astrocyte culture medium was added to quench the trypsin and the suspension transferred to a 15 mL Falcon tube for centrifugation at 1200 rpm for 3 minutes. The supernatant was removed and cells were re-suspended in 2 mL of astrocyte medium. Cells were counted and approximately 30 000 cells in 50 μL were seeded onto non-coated nano-fibers or microgrooves for 4 h before wells were flooded with media. Pre-seeded astrocytes on scaffolds were cultured for 48 h in astrocyte medium. Thereafter, astrocyte medium was removed and E15–16 LGE neurons were seeded at a density of 30 000 cells in 50 μL of NCM and incubated for 2 h before adding sufficient culture media to submerge the constructs. LGE neurons were kept in culture for 7 days before they were fixed and stained.

Immunohistochemistry

Cells were washed in PBS to remove cell debris and medium. They were fixed in 4% paraformaldehyde (PFA, Sigma-Aldrich, Dorset, United Kingdom) for 20 minutes. Cells were washed three times for 5 minutes in tris-buffered saline (TBS, 12 g trizma base from MERCK, Germany, 9 g NaCl, 1 L dH2O). Afterwards, cells were blocked at 4 °C in 5% normal goat serum (NGS) in TBS–T (200 mL TBS and 400 μL triton X-100) for an hour. Primary antibodies: GFAP (2.4 g L^{-1} Anti-Glial Fibrillary Acidic Protein, Dako, UK) and beta-III tubulin (1 mg mL^{-1}, Covance, UK) in 1% NGS, in TBS–T were added to the cultures and left overnight at 4 °C. Cells were washed in TBS three times for 5 minutes. Secondary antibodies (goat anti-mouse fluoprobe 547H and goat anti-rabbit fluoprobe 488 both at dilution ratio of 1 : 300, Interchim) in 1% NGS and TBS–T were added to the cultures that were then stored in the dark at room temperature for 2 hours before washing in TBS. Vectashield hardset mounting medium with DAPI (Vector laboratories, UK) was placed on 22 × 22 mm coverslips (VWR International, UK) and these were then placed upside down onto each construct.

Digital imaging and quantification

A Nikon Eclipse 80i microscope was used to view constructs and ensure that topographical patterns (nano-fibers and micro-grooves) were visible. Images were captured using a Nikon camera and the measurements for processes angles were carried out using NIS Elements (BR3.00, SP3) imaging software. The direction of neurite elongation was measured relative to aligned nano-fibers/grooves. A best line of fit of the longest part of the neurite was drawn and the angle between this line and groove orientation calculated. Angle measurements were collected and were 'binned' into ranges of: 0–10°, 11–20°, 21–30°, 31–40°, 41–50°, 51–60°, 61–70°, 71–80° and 81–90° angles. Two-way analysis of variance (ANOVA) was carried out followed by either Sidak's or Tukey's test for post-hoc multiple comparisons, using GraphPad Prism v6 software. For correlation of the angle of neurite alignment *vs.* groove width treatment Fisher's exact test and least squares regression fitting were performed. Values of $p < 0.05$ were considered significant.

Results and discussion

Neurites responded to topography, particularly on PLL–LN-coated substrates

We fabricated nano and micro-scale topographic structures, PLA nano-fibers and polydimethylsiloxane (PDMS) micro-grooves, using electrospinning and soft lithography techniques, respectively. These techniques and their respective polymers are well established and have been used to fabricate structures designed to provide contact guidance cues.[16] The phenomenon of '*contact guidance*' has been reported in a number of studies and is concerned with the ability of physical structures to direct the orientation of cells.[28–32] Directionally aligned nano-fibers (Fig. 1A), attached to coverslips, had an average diameter of 500 nm.[19] PDMS micro-grooves (Fig. 1B) had width ranging from 20–80 μm and ridges were 5 μm wide and 2.2 μm tall (see ESI†).

Dissociated cells cultured on non-coated substrates (of both nano-fibers and micro-grooves) did not readily attach and had poor viability, *i.e.* cell bodies neither elongated nor produced neurites as expected. This led us to design substrates with a combination of either: topography (nano-fibers or micro-grooves) and (bio)chemical (PLL–LN) cues, based on evidence that these cues promote neuron adherence as well as axon protrusion;[16,33,34] or topography and biological (pre-seeded

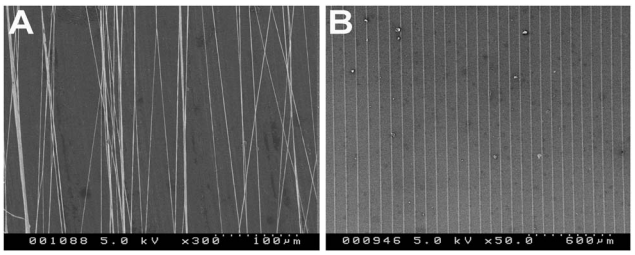

Fig. 1 Topographic cues presented to cells. (A) Aligned PLA nanofibers (B) polydimethylsiloxane (PDMS) micro-grooves.

astrocytes) cues, based on evidence that glial cells provide '*biological topography*' cues to direct neurite orientation.[8,35,36] We studied the viability of primary CNS neurons as well as response of neurites to topography on substrates.

Neurons on all substrates: micro-grooves with PLL–LN (MPL, Fig. 2A), micro-grooves with pre-seeded astrocytes (MpA, Fig. 2B), nano-fibers with PLL–LN (NPL, Fig. 2C) and control (PLL–LN on glass coverslips with no topographic structure, Fig. 2D) had very good attachment and viability. Poly amino acids such as PLL and polyornithine enhance neuronal adhesion by generating a positive charge on substrates creating an electrostatic interaction with the negatively charged membrane.[13,14] Extracellular matrix (ECM) proteins such as laminin, fibronectin and collagen possess multiple binding sites that promote adherence of cells and development of neurites.[13,16,19,37] Neurons were attached to the constructs approximately 2 hours after seeding; it was possible to check morphology of the cells to distinguish neurons from astrocytes at this point (see ESI†). Small neurites were easily noticeable emanating from cell bodies at approximately 24 hours after neurons were seeded. Some processes were not easily observable before immunostaining since they were very fine and for MPL, extending closely along the lower corners of the micro-grooves. Following immunohistochemistry most neuronal cell bodies were observed randomly orientated, but their processes (mainly for single neurons on MPL substrates) were orientated along the topographic structure. The direction of neurite elongation was measured with respect to the topographic pattern, data being binned in terms of the degree of alignment, *e.g.* greater alignment was recorded as a smaller angle between the neurite and surface topography direction. Neurites on control substrates were randomly oriented due to the absence of topography cues, and neurite angles measured on these control coverslips were evenly distributed across all bins, *i.e.* from 0–10° through to 81–90°.

Combination of both topography and (bio)chemical cues had a significant effect on neurite alignment (Fig. 2E; 2 Way ANOVA: $F_{(24,72)} = 13.10$, $p < 0.0001$). This is in agreement with earlier findings.[38] MPL and NPL had the most significant effect on neurite alignment compared to controls (MPL *vs.* control: Tukey, $t = 32.70$, $p < 0.0001$ and NPL *vs.* control: Tukey, $t = 24.27$, $p < 0.0001$). On both micro- and nano-topographies, significantly more neurites were aligned within 0–10° of the

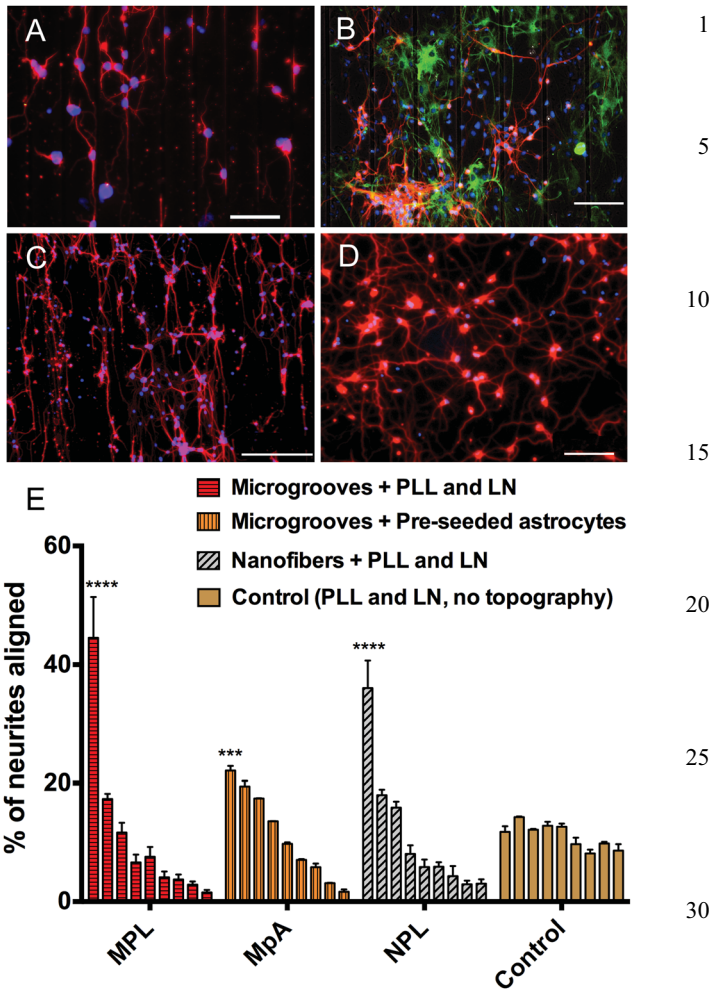

Fig. 2 Fluorescent micrographs indicating the response of neurons cultured on: (A) microgrooves coated with PLL–LN, MPL; (B) micro-grooves coated with astrocytes, MpA; (C) nanofibers coated with PLL–LN, NPL; & (D) control coverslips coated with PLL–LN. Red = β-III-tubulin labeled neurons, green = glial fibrillary acidic protein (GFAP) labeled astrocytes and blue = DAPI stained cellular nuclei. Scale bars: (A–D) = 100 μm. Topographies in panels (A–C) are in the vertical plane with microgrooves clearly visible in (B). (E) Graphs indicating the angle of neurites with respect to topographic direction, from 0–10° (first bar) to 80–90° (final bar) for each treatment. (****, $p < 0.0001$ & ***, $p < 0.001$) indicate significant alignment *vs.* controls.

topographical cue. Approximately 44% of neurites on MPL were angled within 0–10° of the topography and 36% for NPL.

Data analysis demonstrated that PLL–LN coated surfaces preferentially steered neurons to follow substrate micro-grooves (~44% compared with ~12% for the flat control cultures, Tukey, $t = 9.20$, $p < 0.001$); cells on flat surfaces of the control coverslips had randomly oriented axons, with ~1/9th of the population 'orienting' within 10° of a given direction.

Neurons cultured onto a pre-seeded astrocyte layer were found to follow the directionality of the astrocytes more so than the substrate topography. We observed that most of the astrocytes pre-seeded on non-coated micro-grooves failed to attach fully and extend processes. After 48 hours in culture, any attached astrocytes were still spherical; they were mainly

individual cells evenly distributed over the substrate. Neurons were seeded onto astrocytes at 48 hours. After seven days astrocytes were visible in the cultures, had attached and had developed a typical morphology with extended processes (Fig. 2B). Astrocytes on micro-grooves did not show significant alignment of their processes with the grooves. Most neurons cultured on these pre-seeded cells formed colonies, often closely associated with astrocytes, and there was a clear dominant effect to orient neurites towards astrocyte processes rather than to follow the microgroove walls. From our observations, neurites that were aligned, *i.e.* oriented within 0–10° of the micro-grooves, only occurred when they extended from neurons not in contact with astrocytes, these cultures therefore showing an intermediate number of axons orientated to micro-grooves (~21%, Fig. 2E).

We found that astrocytes were highly directionally responsive to non-coated nano-fibers (see ESI†); fibers are more hydrophilic and have a larger surface-area-to-volume ratio compared to micro-grooved structures. However, neurons cultured on astrocytes that were pre-seeded on to nanofibers failed to attach consistently and survive or extend many processes, so no counts were performed.

We compared all substrates with topographic structures against each other to determine whether there was any significant difference amongst them. Substrates with PLL–LN coating (MPL and NPL) showed significantly better alignment of neurites than micro-grooved substrates pre-seeded with astrocytes (MpA), (MPL *vs.* MpA, Tukey, $t = 23.50$, $p < 0.0001$ and NPL *vs.* MpA, Tukey, $t = 15.06$, $p < 0.0001$).

Comparing the two PLL–LN conditions, micro-grooves had more aligned neurites (within 0–10° of the topographical structure) than nano-fibers (Tukey, $t = 8.43$, $p < 0.01$). Approximately 36% of neurites were aligned on NPL substrates compared to 44% on MPL substrates. Aligned micro-grooves had several benefits compared to nano-fibers: they have higher regularity compared to aligned nano-fibers due to the use of templates and the polymer used. Indeed PDMS has been used to culture CNS neurons, in micro-fluidic systems[39,40] where micro-scale grooves are used to direct neurite extension.

Neurite behavior on PLL–LN pre-coated micro-grooves

We discovered that groove height (2.2 μm) restricted, and therefore directed, the orientation of neurites. Studies have reported the influence of groove depth, ranging from 0.2 μm to 15 μm,[33,41] on neurite alignment. Hoffman-Kim *et al.* established a relationship between groove depth and cell alignment or neurite outgrowth.[33] Alignment and outgrowth increased with increase in depth from 0.2 μm to 4 μm; no alignment was observed below 0.2 μm; where neurites almost ignored the topography structure.[33] Increase in groove height correlated to increase in alignment for DRG neurites since they were physically restricted to grooves on which they were located and therefore found it difficult to cross to adjacent grooves.[33,34]

In our study, dissociated cells were spread out such that no clumps or clusters were observed after seeding. However, we discovered that some cells had formed clusters after 7 days in culture; we defined a cluster of cells as being when two or more soma (cell bodies) were located at a distance 20 μm or less than each other. We found that most neurites emanating from single or isolated neurons were much more influenced by topography cues compared to those from clusters of two or more neurons (Fig. 3A–C). Neurites from 'single' neurons were significantly better aligned to microgrooves (Single *vs.* cluster: Sidaks, $t = 44.95$, $p < 0.0001$) than neurites from clusters of neurons. We believe that orientation of neurites from clusters was influenced more by cues from close by cells rather than topography cues.

Since we cultured dissociated cells on micro-grooved substrates with varying groove width we examined if alignment of neurites extending from soma was affected by changes in groove width. We chose a lower limit of 20 μm to allow sufficient space to accommodate the soma of astrocytes and neurons adjacent to one another within a single groove; and an upper limit of 80 μm to allow for soma to reside within the centre of grooves without any direct contact with groove walls. Neurite orientation did not correlate to groove width (Fig. 4, $r^2 = 0.0284$, $p < 0.0001$). We believe this was due to most cells extending neurites that followed groove walls after contact, regardless of where the cell soma was located within the groove, their processes finding a groove edge and then extending along this. This finding is somewhat contrasting to reports from other studies. In general, it has been shown that groove or microchannel width influences alignment. Alignment of PC12 neurites reduced from 90% to 75% when the width of gratings

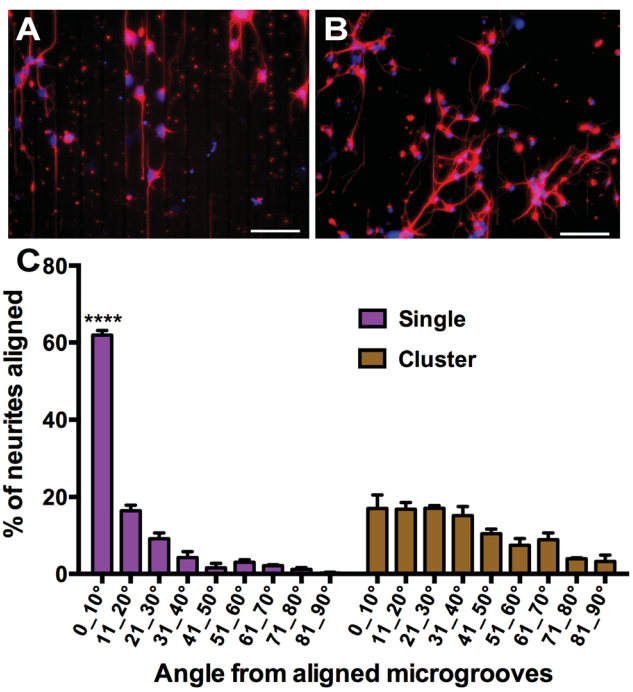

Fig. 3 Neuronal culture on PLL–LN-coated microgrooves. Neurites from single cells, (A), are more responsive to microgrooves than neurites from clusters, (B). Red = β-III-tubulin labeled neurons and blue = DAPI stained cellular nuclei. Scale bars = 100 μm. (C) Quantification of angle of neurites with respect to topographic direction. (****, $p < 0.0001$) indicates significant alignment of neurites from single cells *vs.* clusters.

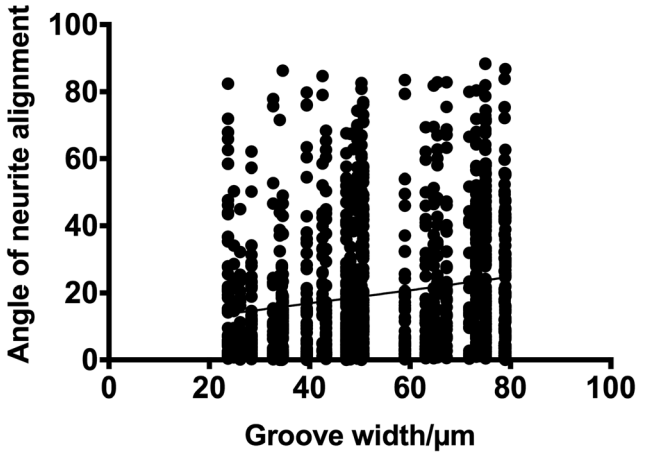

Fig. 4 Neurite alignment on grooves pre-coated with PLL–LN (MPL) was independent of groove width. Black dots represent individual neurite angles measured. Line of best fit $R^2 = 0.0284$, indicating no correlation.

200 nm deep was reduced from 750 nm to 500 nm.[42] When the same cell type was cultured on 23 μm deep substrates with 5 μm and 10 μm widths, more alignment was observed on 5 μm wide stripes.[43] Furthermore, polyimide patterns with height of 11 μm and width ranging from 20–60 μm showed that all widths were effective in guiding neurite orientation, however more significant alignment was observed on smaller channels of 20–30 μm width.[44] Therefore, cell response to groove width may be strongly dependent on the cell type as well as the topography.

Conclusions

In this study we have demonstrated the sensitivity of primary CNS neurons to nano- and micro-scale topographic features and the dependence of supporting astrocytes and cell–cell communication to direct neurite outgrowth. Contact guidance cues showed a positive control over neurite orientation, although clustered cells tended to follow their own, more dominant biochemical signalling cues. The results presented here clearly demonstrate the potential to control primary neuronal cultures *in vitro* using surface engineered approaches, and highlights the interaction of cell–cell signalling as a key contributing factor in the preparation of oriented neural constructs. This work advances our ability to generate robust and reproducible models of neurodegenerative disease *in vitro*, with the potential to advance our capabilities for regenerative medicine in the CNS.

Acknowledgements

This work was carried out through funding from EPSRC DTC in Regenerative Medicine, UK EP/F500491/1.

Notes and references

1 L. Cote and M. D. Crutcher, Basal Ganglia Components, in *Principles of Neural Science*, ed. E. R. Kandel, J. H. Schwartz and T. M. Jessell, Prentice-Hall International Inc., 3rd edn, 1991, ch. 42, pp. 647–658.
2 J. A. Obeso, M. C. Rodriguez-Oroz, M. Stamelou, K. P. Bhatia and D. J. Burn, *Lancet*, 2014, **384**, 523–531.
3 P. Roach, T. Parker, N. Gadegaard and M. R. Alexander, *Biomater. Sci.*, 2013, **1**, 83–93.
4 H. Wichterle, D. H. Turnbull, S. Nery, G. Fishell and A. Alvarez-Buylla, *Development*, 2001, **128**, 3759–3771.
5 K. Kalil and E. W. Dent, *Curr. Opin. Neurobiol.*, 2005, **15**, 521–526.
6 R. A. Fricker-Gates, *NeuroReport*, 2006, **17**, 1081–1084.
7 E. East, D. B. de Oliveira, J. P. Golding and J. B. Phillips, *Tissue Eng., Part A*, 2010, **10**, 3173–3178.
8 J. B. Recknor, J. C. Recknor, D. S. Sakaguchi and S. K. Mallapragada, *Biomaterials*, 2004, **25**, 2753–2767.
9 J. K. Alexander, B. Fuss and R. J. Colello, *Neuron Glia Biol.*, 2008, **2**, 93–103.
10 J. Raper and C. Mason, *Cold Spring Harbor Perspect. Biol.*, 2010, **2**, a001933.
11 S. Xing, W. Liu, Z. Huang, L. Chen, K. Sun, D. Han, W. Zhang and X. Jiang, *Electrophoresis*, 2010, **31**, 3144–3151.
12 R. Murugan, P. Molnar, K. Rao and J. Hickman, *J. Biomed. Eng.*, 2009, **2**, 104–134.
13 S. Khan and G. Newaz, *J. Biomed. Mater. Res., Part A*, 2010, **93**, 1209–1224.
14 T. G. Ruardij, M. H. Goedbloed and W. L. Rutten, *IEEE Trans. Biomed. Eng.*, 2000, **47**, 1593–1599.
15 A. Chan, R. P. Orme, R. A. Fricker and P. Roach, *Adv. Drug Delivery Rev.*, 2012, **65**, 497–514.
16 Y. Liu, Y. Sun, H. Yan, X. Liu, W. Zhang, Z. Wang and X. Jiang, *Small*, 2012, **8**, 676–681.
17 P. Weiss, *Yale J. Biol. Med.*, 1947, **19**, 235–278.
18 P. Weiss, *J. Exp. Zool.*, 1945, **100**, 353–386.
19 P. Roach, T. Parker, N. Gadegaard and M. R. Alexander, *Surf. Sci. Rep.*, 2010, **65**, 145–173.
20 Y.-S. Lee and T. Livingston Arinzeh, *Polymers*, 2011, **3**, 413–426.
21 T. J. Sill and H. A. von Recum, *Biomaterials*, 2008, **29**, 1989–2006.
22 W. Liu, S. Thomopoulos and Y. Xia, *Adv. Healthcare Mater.*, 2012, **1**, 10–25.
23 J. E. Petrzelka and D. E. Hardt, *J. Micromech. Microeng.*, 2012, **22**, 075015.
24 Y. Xia and G. M. Whitesides, *Annu. Rev. Mater. Sci.*, 1998, **28**, 153–184.
25 R. Bashir, *Adv. Drug Delivery Rev.*, 2004, **56**, 1565–1586.
26 Y. Yang, I. Wimpenny and M. Ahearne, *Nanomedicine: Nanotechnology, Biology, and Medicine*, 2011, **7**, 131–136.
27 S. B. Dunnett and A. Björklund, Staging and dissection of rat embryos, in *Neural transplantation a practical approach*, ed. S. B. Dunnett and A. Björklund, IRL Press, Oxford, 1992, ch. 1, pp. 1–18.
28 I. Nagata, A. Kawana and N. Nakatsuji, *Development*, 1993, **117**, 401–408.
29 A. Rajnicek, S. Britland and C. McCaig, *J. Cell Sci.*, 1997, **110**(Pt 2), 2905–2913.

30 N. Gomez, S. Chen and C. Schmidt, *J. R. Soc., Interface*, 2007, **4**, 223–233.
31 C. Chou, A. Rivera, T. Sakai, A. Caplan, V. Goldberg, J. Welter and H. Baskaran, *Tissue Eng., Part A*, 2013, **19**, 1081–1090.
32 I. Tonazzini, S. Meucci, P. Faraci, F. Beltram and M. Cecchini, *Biomaterials*, 2013, **34**, 6027–6036.
33 D. Hoffman-Kim, J. A. Mitchel and R. V. Bellamkonda, *Annu. Rev. Biomed. Eng.*, 2010, **12**, 203–231.
34 C. Miller, S. Jeftinija and S. Mallapragada, *Tissue Eng.*, 2002, **8**, 367–378.
35 R. Deumens, G. C. Koopmans, C. G. J. Den Bakker, V. Maquet, S. Blacher, W. M. M. Honig, R. Jérôme, J. P. Pirard, H. W. M. Steinbusch and E. A. J. Joosten, *Neuroscience*, 2004, **125**, 591–604.
36 E. East, D. B. de Oliveira, J. P. Golding and J. B. Phillips, *Tissue Eng., Part A*, 2010, **16**, 3173–3184.
37 K. M. Gladwin, R. L. D. Whitby, S. V. Mikhalovsky, P. Tomlins and J. Adu, *Adv. Healthcare Mater.*, 2013, **2**, 728–735.
38 Y. Sun, Z. Huang, W. Liu, K. Yang, K. Sun, S. Xing, D. Wang, W. Zhang and X. Jiang, *Biointerphases*, 2012, **7**, 29.
39 D. Majumdar, Y. Gao, D. Li and D. Webb, *J. Neurosci. Methods*, 2011, **196**, 38–44.
40 A. M. Taylor, M. Blurton-jones, S. W. Rhee, D. H. Cribbs and W. Carl, *Nat. Methods*, 2005, **2**, 599–605.
41 H. Francisco, B. B. Yellen, D. S. Halverson and G. Friedman, *Biomaterials*, 2007, **28**, 3398–3407.
42 M. Cecchini, A. Ferrari and F. Beltram, *J. Phys.: Conf. Ser.*, 2008, **100**, 012003.
43 L. Yao, S. Wang, W. Cui, R. Sherlock, C. O'Connell, G. Damodaran, A. Gorman, A. Windebank and A. Pandit, *Acta Biomater.*, 2009, **5**, 580–588.
44 M. J. Mahoney, R. R. Chen, J. Tan and W. M. Saltzman, *Biomaterials*, 2005, **26**, 771–778.